Hydrol. Earth Syst. Sci. Discuss., https://doi.org/10.5194/hess-2017-689
Manuscript under review for journal Hydrol. Earth Syst. Sci.
Discussion started: 2 January 2018

Hydrology and Earth System Sciences
Discussions

Evaluation of Doppler radar and GTS Data Assimilation for NWP Rainfall Prediction of an Extreme Summer Storm in Northern China: from the Hydrological Perspective

Jia Liu[1], Jiyang Tian[1], Denghua Yan[1], Chuanzhe Li[1], Fuliang Yu[1], Feifei Shen[2]

[1] State Key Laboratory of Simulation and Regulation of Water Cycle in River Basin, China Institute of Water Resources and Hydropower Research, Beijing, 100038, China
[2] Key Laboratory of Meteorological Disaster of Ministry of Education, Nanjing University of Information Science & Technology, Nanjing, 210044, China

Correspondence to: Jia Liu (hettyliu@126.com)

Abstract. Data assimilation is an effective tool in improving high-resolution rainfall of the numerical weather prediction (NWP) systems which always fails in providing satisfactory rainfall products for hydrological use. The aim of this study is to explore the potential effects of assimilating different sources of observations from the Doppler weather radar and the Global Telecommunication System (GTS) in improving the mesoscale NWP rainfall products. A 24 h summer storm occurring over the Beijing-Tianjin-Hebei region of northern China on 21 July 2012 is selected in this study. The Weather Research and Forecasting (WRF) model is used to obtain 3 km rainfall forecasts, and the observations are assimilated using the three-dimensional variational (3D-Var) data assimilation method. Eleven data assimilation modes are designed for assimilating different combinations of observations in the two nested domains of the WRF model. Results show that the assimilation can largely improve the WRF rainfall products especially the accumulative process of rainfall, which is of great importance for hydrologic applications through the rainfall-runoff transformation process. Both radar reflectivity and GTS data are good choices for assimilation in improving the rainfall products, whereas special attentions should be paid for assimilating radial velocity where unsatisfactory results are always found. Simultaneously assimilating GTS and radar data always perform better than assimilating radar data alone. The inclusion of GTS data in the nested domains when radar reflectivity and radial velocity are assimilated in the innermost domain show the best results among all the 11 assimilation modes. The assimilation efficiency of the GTS data is higher than both radar reflectivity and radial velocity considering the number of data assimilated and its effect. It is also found that the assimilation of more observations cannot guarantee further improvement of the rainfall products, whereas the effective information contained in the assimilated data is of more importance than the data quantity. Potential improvements of data assimilation in improving the NWP rainfall products are discussed and suggestions are also made.

Hydrol. Earth Syst. Sci. Discuss., https://doi.org/10.5194/hess-2017-689
Manuscript under review for journal Hydrol. Earth Syst. Sci.
Discussion started: 2 January 2018

Hydrology and Earth System Sciences
Discussions

1 Introduction

Numerical weather prediction (NWP) systems play an important role in the prediction of meteorological and hydrological processes with the ability of providing relatively reliable products for analyzing and forecasting weather events (Rodwell et al, 2010; De et al, 2011; Boussetta et al, 2013). Rainfall is not only a crucial meteorological variable but is also a hydrological element; therefore, it is always important to obtain accurate rainfall information for hydrological use. Unfortunately, because of the uncertainties and complexities of atmospheric processes, rainfall is among the most difficult variables to be accurately captured using NWP (Berenguer et al, 2012; Shrestha et al, 2013). The Weather Research and Forecasting (WRF) model is a latest generation mesoscale NWP system that has been widely used for rainfall simulation and prediction (Efstathiou et al, 2013; Yang et al, 2015). Although rainfall products can be directly used due to the high accuracy of rain or no rain predictions, the WRF model still cannot ensure accurate rainfall quantities or spatiotemporal distributions at the catchment scale for hydrological prediction (Liu et al, 2012; Li et al, 2013).

Qie et al. (2014) simulated a storm event that featured short-term (12 h) heavy rainfall and frequent lightning activity over northern China using the WRF model. The results showed that the mean absolute error of the 6 h accumulated rainfall was 39.8 mm for an observed rainfall range of 20-50 mm, whereas the mean absolute error reached 53.3 mm for an observed rainfall range of 11-20 mm. Hamill (2014) used an ensemble prediction system to analyze the performance of the WRF model in northern Colorado. Although ensemble prediction could avoid the complications induced by uncertainties, the accumulated rainfall also had a large bias compared with the observations. Kryza et al. (2013) found that the WRF model always underestimated the 24 h accumulated rainfall in Poland, and the rainfall coverage area greatly changed based on different physical parameterizations. Efstathiou et al. (2013) indicated that the WRF model could not capture the maximum rainfall intensity in either time or space at Chalkidiki, Greece. Gascón et al. (2016) used the WRF model to simulate an exceptionally heavy convective rainfall on 3 July 2006 in Calabria, Italy. The simulation results were unsatisfactory, and the total rainfall was significantly underestimated.

Data assimilation has been shown to be an efficient way in improving the quality of the WRF rainfall products (Liu et al, 2013). The WRF model provides a three dimensional-variational data assimilation system, i.e., WRF-3DVar (Barker et al, 2004), that works in tandem with the WRF model in real-time. The system can assimilate various types of conventional and non-conventional data, such as observations from surface weather stations, buoys, ships, pilot balloons, radars and satellites (Routray et al, 2010). Many studies have shown that WRF-3DVar works well with observations from different sources. Routray et al. (2012) assimilated upper-air and surface data from the Global Telecommunication System (GTS) using WRF-3DVar, and the results showed that the location and amount of rainfall was captured better over the west coast of India when compared with the simulation without data assimilation. Wind observations were also assimilated using WRF-3DVar as the main observed data for rainfall simulation in India, and the rainfall intensity and spatial distribution were considerably improved (Mohanty et al, 2012). To improve heavy rainfall forecasts over the Korean Peninsula, global positioning system

(GPS) radio occultation (RO) data were used with WRF-3DVar (Ha et al, 2014). Results indicated that the quantitative accuracy of the rainfall forecast was in better agreement with observations, especially the maximum rainfall amount.

Compared with other observational data, Doppler radar can obtain detailed rainfall information with spatial resolutions of a few kilometers and temporal resolutions of a few minutes (Sugimoto et al, 2009). With high spatial and temporal resolutions, Doppler radar can reveal detailed structural features of mesoscale storms and capture rapidly developing convective weather systems (Pu et al, 2009; Maiello et al, 2014). Moreover, Doppler radar can provide real-time observations that can be assimilated using WRF-3DVar and used for real-time rainfall forecasts (Liu et al, 2013). Some studies have also indicated that significant improvements could be obtained in rainfall simulations using data assimilation (Bauer et al, 2015), because radar data can provide more detailed information on the initial fields and improve the lateral boundary conditions of the WRF model (Sokol and Pešice, 2009).

Doppler radar can provide two types of observations for assimilation, i.e., radar reflectivity and radial velocity. Both have been found to have positive impacts on NWP rainfall simulations and forecasts, especially for heavy rainfall events (Li et al, 2012). Based on the operating principle of Doppler radar, reflectivity contains information on the number of falling drops per unit volume, which depends on the hydrometeor number and size, whereas radial velocity is related to vertical atmospheric motions (Maiello et al, 2014). This means that assimilating reflectivity impacts the thermodynamic and dynamic fields, whereas radial velocity assimilation only influences the dynamic fields (Xiao and Sun, 2007; Abhilash et al, 2012). Li et al. (2012) indicated that assimilating radial velocity every 30 min could improve the accuracy of rainfall (caused by hurricane) intensity prediction. Sun et al. (2012) found that the pattern and location of forecasted rainfall were noticeably improved with radar reflectivity assimilation. Pan et al. (2012) found that the WRF model can capture rainfall distributions in time and space better by assimilating both Doppler radar reflectivity and radial velocity. Abhilash et al. (2012) went further and compared the assimilation effects of radar reflectivity and radial velocity. Results showed that the assimilation of both radar reflectivity and radial velocity significantly improved most meteorological elements, including wind, temperature, moisture and rainfall.

However, it has been found that data assimilation is mainly used for synoptic analyses of meteorological fields. The potential of data assimilation has not been fully studied for hydrological purposes, which require a more rigorous evaluation of rainfall quantities and variations (Liu et al, 2015). Rainfall prediction is especially important for real-time flood forecasting in small sized catchments which often have short concentration times and need predicted rainfall to extend the flood forecast lead time (Liu and Han, 2013). Therefore, hydrologists are particularly concerned about the accuracy of the accumulative amount and the process of the predicted rainfall at the catchment scale. The rainfall process directly impacts the forecasted discharge and the timing of the flood peak through rainfall-runoff transformation modeling. To what extent can the assimilation of Doppler radar observations help improve rainfall predictions of particular storm events at the catchment scale? Is it always the best choice to simultaneously assimilate radar reflectivity and radial velocity? In general, Doppler radar is easily contaminated by non-weather returns, such as second-trips, sidelobe clutter, gound clutter and low signal-to-noise returns, which can affect the quality of radar data and the assimilation effect (Zhang et al, 2012). Therefore, it may be of interest to

examine whether rainfall predictions can be improved by assimilating radar data with other observations, such as meteorological elements from fixed and mobile stations.

A 24 h storm event that occurred in July of 2012 in the Beijing-Tianjin-Hebei region of northern China was selected for this study. The storm event has received wide attention due to its high intensity and the significant losses caused by the corresponding flooding. The 24 h rainfall that accumulated in the small mountainous catchment of Zijingguan, which has a drainage area of 1760 km^2, was regenerated using the WRF model with different data assimilation scenarios. Observations from an S-band Doppler weather radar that completely covers the Zijingguan catchment were assimilated with the assistance of WRF-3DVar. Traditional meteorological data from the GTS were obtained from the National Center of Atmospheric Research (NCAR). Eleven different data assimilation modes were designed for assimilating different combinations of the three types of data, i.e., radar reflectivity, radial velocity and GTS observations, in the two nested domains of the WRF model. The improvements in the forecasted rainfall from the 11 data assimilation scenarios were evaluated from the perspectives of the accumulative process and total quantity. The performances of different data assimilation scenarios are compared, and the efficient way to assimilate Doppler radar observations for rainfall prediction is further discussed.

2 The WRF model and 3D-Var data assimilation

2.1 The WRF model setup

The WRF model (version 3.6) is a next-generation meteorological model that includes a variety of physical options and can be used over a wide range of scales, ranging from tens of meters to thousands of kilometers. Detailed descriptions of the model were available in Skamaraock et al. (2008). Two nested domains were centered over the Zijingguan catchment, and two-way nesting was used for communication between the parent and child domains. To obtain high-resolution rainfall products and make the results applicable for hydrological forecasting systems, the horizontal grid spacing of the WRF inner domain (Domain 2) was set to 3 km, and the downscaling ratio was set to 1:3 (Yang et al, 2012; Chambon et al, 2014). The nested domain sizes were 1260×1260 and 450×360 km^2 for the Zijingguan catchment. The two domains were comprised of 40 vertical pressure levels, with the top level set to 50 hPa. The model initial and lateral boundary conditions were obtained from Global Forecast System (GFS) forecast data, which were provided by NCEP with 1°×1° grids and were widely used to forecast historical storm events (Routray et al, 2010; Ha and Lee, 2012). The time step of the WRF model output was set to one hour. Considering the use of downscaling and the high resolution needed for meteorological and hydrological studies, the forecasted rainfall in the inner domain was chosen for analysis.

Cumulus physics, microphysics and planetary boundary layer (PBL) are important physical parameterization options for rainfall simulations (Cassola et al, 2015; Fernández-González et al, 2015). Considering the performance of the physical parameterizations in northern China, Kain-Fritsch (KF) for cumulus physics, WRF single-moment 6 (WSM6) for microphysics and Mellor-Yamada-Janjic (MYJ) for PBL were adopted for this study (Miao et al, 2011; Guo et al, 2014; Di et al, 2015).

Hydrol. Earth Syst. Sci. Discuss., https://doi.org/10.5194/hess-2017-689
Manuscript under review for journal Hydrol. Earth Syst. Sci.
Discussion started: 2 January 2018

2.2 3-DVar data assimilation

The 3-DVar data assimilation produces an optimal estimate of the atmospheric state through iterative solution of a prescribed cost function (Ide et al, 1997):

$$J(x)=\frac{1}{2}(x-x^b)^T B^{-1}(x-x^b)+\frac{1}{2}(y-y^0)^T R^{-1}(y-y^0) \quad (1)$$

where x is the atmospheric and surface state vector, x^b is the first guess or background, and y^0 is the assimilated observation. y is the observation space derived from the model. $\boldsymbol{B}$ and $\boldsymbol{R}$ are the background error covariance matrix and the observation error covariance matrix, respectively.

The WRF-3DVar data assimilation system in the WRF model was used for assimilating the GTS and weather radar data in real-time (Barker et al, 2004; Gao et al, 2004). The background error covariance CV3 was used in this study. The greatest advantage of CV3 is its wide applicability (Meng and Zhang, 2008). The reason why CV3 is used also includes the trial to simplify the data assimilation procedure which enables a more extensive application among hydrologists.

3 Study area and data

3.1 Study area and storm event

The Zijingguan catchment, which lies in the northern reach of the Daqing river basin, was chosen as the study area (Fig. 1). It is located at 39°13′~ 39°40′ north latitude and 114°28′~115°11′ east longitude and has a drainage area of 1760 km^2. It is 54 km long from north to south and 61 km wide from east to west. The Zijingguan catchment has a temperate continental monsoon climate. The average annual rainfall is approximately 600 mm, and the majority of rain falls during the flood season from late May to early September. The size and terrain together with the previous history of extreme storms and floods make the Zijingguan catchment representative of the catchments in the semi-humid and semi-arid area of northern China that require flood warnings. To avoid enormous losses caused by floods, accurate rainfall forecasts are very important.

[Figure 1]

A 24 h storm event that occurred over the Beijing-Tianjin-Hebei region on 21 July 2012 was chosen for this study. Because of the high intensity rainfall, wide coverage and significant losses, the storm event has received widespread attention in China. The 24 h accumulated rainfall with 172 mm led to the high peak flow (2580 m^3 s^{-1}) in the Zijingguan catchment. The observed areal rainfall in the Zijingguan catchment can be calculated using the Thiessen polygon method with the rainfall data from the 11 rain gauges, which were chosen as the ground truth to evaluate the WRF outputs. If more than 50% of a grid cell was covered by the Zijingguan catchment, the rainfall data from that grid cell were chosen to calculate the forecasted areal rainfall using the average values. The 11 rain gauges with the Thiessen polygons and the model grid cells (3 km × 3km) were shown in Fig. 1.

Hydrol. Earth Syst. Sci. Discuss., https://doi.org/10.5194/hess-2017-689
Manuscript under review for journal Hydrol. Earth Syst. Sci.
Discussion started: 2 January 2018

3.2 GTS data

Surface weather station, ship, buoy, pilot balloon, sonde, aircraft and satellite observations from the GTS were processed using the OBSPROC observation preprocessor before being assimilated using WRF-3DVar. A shell script was compiled to transform the decoded data to the suitable LITTLE_R format, which can be directly used by WRF-3DVar for data assimilation. Wide coverage in horizontal direction and high levels in vertical direction are the main characteristic of the GTS data, although the spatial density of the observations was low, and the time interval of the GTS data was 6 h. Therefore, the GTS data are usually used to improve the prediction of large-scale flows.

The quality control of the GTS data is implemented in WRF-3DVar by defining the observation error covariance. The default US Air Force (AFWA) OBS error file is used in this study, which defines the instrumental and sensor errors for various air, water and surface observation types as well as satellite retrievals.

3.3 Weather radar data

An S-band Doppler weather radar is located in Shijiazhuang, the capital of Hebei province. It is approximately 100 km from the Zijingguan catchment and covers a radius of 250 km. The study area can be completely covered by the radar. The radar cycles include 9 different scan elevations every 0.1 h over the course of a day. Figure 2 shows the relative positions of the WRF domains and the radar scan area. To make the atmospheric motions more stable and reduce the nonlinearity in the outer domain, radar data were only assimilated in Domain 2 in this study.

[Figure 2]

The S-band radar belongs to the newest generation weather radar network of China (CINRAD/SC), the quality control of which is supported by China Integrated Meteorological Information Service System (CIMISS) of China Meteorological Administration. The potential error sources, such as ground clutter, radial interference echo, speckles and other artefacts, were removed through the quality control procedure (Tong and Xue, 2005). The rainfall observations from rain gauges and weather radar were also compared to check the quality of the radar data. The following Z-R relationship was used to convert the radar reflectivity into rainfall rates (Hunter, 1996):

$$Z = 300 \times R^{1.4} \quad (2)$$

where Z is the radar reflectivity in $mm^6\ m^{-3}$ and R is the rainfall rate in $mm\ h^{-1}$. Figure 3 showed the time series bars and the spatial distributions of the 24 h accumulated rainfall. The accumulated areal rainfall was 160.48 mm observed from the weather radar and 172.17 mm from the rain gauges. Although the accumulated rainfall was slightly underestimated by the weather radar, the spatial distribution of the accumulation was quite consistent with the rain gauges. The temporal variation of the catchment areal rainfall also showed a consistent trend with the rain gauge observations. Therefore, the assimilation of the weather radar data is expected to have positive effect in improving the WRF forecasting results.

[Figure 3]

3.4 Mode configurations

To explore the effects of data assimilation using WRF-3DVar for rainfall prediction in the study area, 11 modes were designed based on the different combinations of the available GTS data, radar reflectivities and radial velocities in the two nested domains, as shown in Table 1. The improvements in the rainfall forecasts using data assimilation with the 11 modes were examined in this study and are shown in Table 1. Besides the different data assimilation combinations, the 11 modes have the same settings of the WRF model and the WRF-3DVar. The purpose of the mode design was to find the most effective way to assimilate the weather radar and traditional meteorological data for improving the WRF rainfall forecasts.

[Table 1]

3.3 Cycling the WRF-3DVar runs

WRF-3Dvar needs to be run in the cycling mode to continuously assimilate real-time observations during storm events. Figure 4 shows the start and end times of the storm event that occurred on 21 July 2012 and the time bars of the cycling WRF-3DVar runs. The storm event began at 03:00 on 21 July 2012 and lasted for 24 h. Data assimilation began at 00:00 on 21 July 2012 and ended at 00:00 on 22 July 2012, with a time interval of 6 h. Thus, the data assimilation took place on four occasions (21/07/2012 00:00, 06:00, 12:00, 18:00 and 00:00). A 6 h spin-up period was executed by run1 and the first-guess files generated in run1 were used for run2. As time progressed, run3, run4, run5 and run6 were initiated at the corresponding times with the first-guess files generated by the previous runs. In the six runs, only run1 was the original WRF run without assimilating observations, which can be treated as a benchmark to evaluate the improvements using data assimilation.

[Figure 4]

4 Results

4.1 4.1 Evaluation of the storm process improvements

Figure 5 shows the cumulative curves of the Zijingguan catchment areal rainfall for the different data assimilation modes. The rainfall process can be easily identified by the cumulative curves. To show the influence of the six runs on the rainfall forecast, all of the WRF-3DVar runs are shown in Fig. 5. The total run time was 36 h, which was longer than the duration (24 h) of the storm event. In Fig. 5, the gray area indicates the duration of the storm event. The black solid line indicates the ground truth of the catchment areal rainfall, which was calculated from the rain gauge observations using the Thiessen polygon method. The six runs are all shown by combining the solid and dashed lines. The solid line segment at the beginning of each run represents a new data assimilation run that generated the most recently updated forecasts. After 6 h, which marks the beginning of the next data assimilation run, the previous run is shown as a dashed line, indicating that the results are no longer the latest. For a given run, the solid and dashed line segments are the same color. The purpose of the data assimilation

was to improve the accuracy of the rainfall forecast, and the presumed trends in the cumulative rainfall from the cycling WRF-3DVar runs should therefore have increasingly approached the black solid line. In reality, the different modes showed different data assimilation effects, and some of them were greatly different from the presumed trends.

Comparing the red and black curves, the original forecast of the areal rainfall accumulation was significantly lower than the ground truth. This finding indicates that the WRF model was unable to forecast the storm event accurately without data assimilation, and the forecasts had negative errors in the accumulated areal rainfall. The forecast errors may lead to poor runoff forecasts due to error accumulation and magnification during the rainfall-runoff transformation process. The rainfall forecasts predicted the onset 6 h earlier than the observations for all 11 modes, although the rainfall accumulations were all less than 20 mm during this period.

Comparing the first three subfigures of Fig. 5, a significant improvement in the accumulated areal rainfall was found in Mode 1 by assimilating the radar reflectivity in Domain 2. The results of Modes 2 and 3 were unstable in the different cycling WRF-3DVar runs, which was a result of the assimilation of the radar velocity data. For Modes 2 and 3, the accumulated areal rainfall forecasts for the first 6 h of run3 were less than for Mode 1, and the assimilation results of run4 were also unsatisfactory. The forecasted rainfall for Modes 2 and 3 was even less than the original run (run1), which did not assimilate observations. This indicates that the assimilation of radial velocity observations at the time 21/07/2012 06:00 and 12:00 was unable to help trigger the main storm process.

For Modes 4 and 5 shown in Fig. 5d and 5e, assimilating the GTS data improved the rainfall forecasts, and only assimilating the GTS data in Domain 1 (Mode 4) was better than assimilating the GTS data in both nested domains (Mode 5). The accumulated areal rainfall of run4 for Mode 4 was higher than for Mode 5, and Mode 4 therefore had better forecasted rainfall than that of Mode 5. This finding indicates that when the two-way nesting was allowed, adding the GTS data at time 21/07/2012 12:00 to Domain 2 for data assimilation may have led to a data conflict with the assimilated GTS data over a large area (Domain 1), which may be the reason that Mode 5 exhibited less improvement than Mode 4. However, the accumulated areal rainfall forecast for Mode 4 was only slightly better than that of Mode 1, although the rainfall processes were very different. For Mode 1, the greatest rainfall amounts were obtained in run3, whereas the rainfall amounts of run4 had the largest proportion for Mode 4. Different types of data assimilation can not only affect the rainfall amounts but also the rainfall process.

In comparison with only assimilating the radar data in Domain 2 (Modes 1, 2 and 3), assimilating the GTS data in Domain 1 as well as the radar data in Domain 2 (Modes 6, 7 and 8) improved the rainfall forecast. For the six modes, the rainfall processes were relatively similar for run1, run2, run5 and run6, whereas the forecasts of run3 and run4 were very different. The accumulated rainfall for run3 in Mode 1 was slightly higher than in Mode 6, whereas the result was opposite for run4. In comparison with Modes 2 and 3, Modes 7 and 8 had larger accumulated rainfall totals in run3 and run4, respectively. This finding indicates that the assimilation of the GTS data in Domain 1 could have affected the rainfall forecast when assimilating radar data in Domain 2, which resulted in further improved forecasts that agreed better with the observed rainfall.

Modes 9, 10 and 11 were designed to explore the influence of the assimilation of the GTS data in Domain 2 on Modes 6, 7 and 8. The results show that the forecasted rainfall for Mode 11 was better than that of Mode 8, whereas Modes 9 and 10 performed worse than Modes 6 and 7, respectively. The accumulated rainfall for run4 in Mode 9 was less than in Mode 6, which indicates that assimilating the GTS data in Domain 2 at 21/07/2012 12:00 may have changed the atmospheric state and water vapor transport when the GTS data were also assimilated in Domain 1 and the radar reflectivity data were assimilated in Domain 2 at the same time. Both run3 and run4 of Mode 10 had much less forecasted rainfall than Mode 7, and the rainfall forecast was the worst among the 11 modes. This result shows that assimilating the GTS data in Domain 2 may have reduced the improvement in the rainfall forecast when the GTS data were also assimilated in Domain 1 and the radial velocity data were assimilated in Domain 2. Unlike Modes 9 and 10, Mode 11 performed better than Mode 8; this mode exhibited the best rainfall forecast. Run4 of Mode 11 predicted more rainfall than the other modes and provided the largest contribution to the 24 h accumulated areal rainfall, which means that the assimilation of the GTS data as well as the two types of radar data at 21/07/2012 12:00 in Domain 2 provided an improved estimate of the atmospheric state.

Mode 6 can be regarded as a combination of Modes 1 and 4. The rainfall evolution of Mode 6 was much closer to that of Mode 4 than that of Mode 1. The same results can be obtained by comparing Modes 2, 4 and 7 as well as Modes 3, 4 and 8. This finding indicates that assimilating the GTS data in Domain 1 affected the rainfall forecast more than assimilating the radar data in Domain 2. Although the area of the Zijingguan catchment is limited, assimilating these data was necessary in improving the atmospheric motion at the large scale.

[Figure 5]

4.2 Evaluation of the 24 h accumulated areal rainfall

To more quantitatively evaluate the 11 data assimilation modes, the accumulated areal rainfall in the Zijingguan catchment was calculated for the 24 h duration of the storm event on 21 July 2012. The rain gauge observations, WRF model forecasts, and relative errors between them are shown in Table 2. For all 11 modes, the first six hours of the runs (solid line segments in Fig. 5), which cover the duration of the storm, were used to calculate the 24 h accumulated areal rainfall.

[Table 2]

The WRF model forecasts without data assimilation were too poor to be used for hydrological forecasting. The forecasted rainfall accumulation was only 95.54 mm, which was much lower than the rain gauge observations, and the relative error was -44.51%. Data assimilation was used to improve the rainfall forecasts, although the forecast results worsened in Modes 2, 3 and 10, and all of the relative errors exceeded 50%. Interestingly, all three modes assimilated radar velocity data. For the other eight modes, the rainfall forecasts were improved at different levels. Mode 11 performed the best because the forecast (165.68 mm) was closest to the rain gauge observation (172.17 mm), and the relative error was only -3.77%. Although Mode 5 was improved by assimilating the GTS data in both nested domains, the effect was the least profound.

Comparing Modes 1, 2, 3, and 4, which all assimilated the observations in a single domain, the lower relative errors were found in Modes 1 (-30.93%) and 4 (-25.06%), whereas the highest error was found in Mode 2 (-54.90%). This finding

indicates that only assimilating the GTS data in Domain 1 was the best choice, and assimilating radar reflectivity in Domain 2 also provided good results. However, only assimilating radar velocity in Domain 2 or assimilating both types of radar data in Domain 2 made the rainfall forecast unsatisfactory. The observation errors in the radial velocity may have been the main factor that led to the poorest performance (Abhilash et al, 2012). Another reason is that assimilating radial velocity can only change the dynamic field, which changes quickly for small-scale regions, and 6 h may have been too long for the assimilation time interval (Lin et al, 2011).

Modes 6, 7 and 8 were formed by assimilating the GTS data in Domain 1 based on Modes 1, 2 and 3. The results show that the relative errors decreased significantly when the GTS data were assimilated in Domain 1. The forecasted rainfall amounts for Modes 6, 7 and 8 were very similar, and the relative errors were all approximately -20%. This finding indicates that assimilating the GTS data over a large area (Domain 1) had large positive effects on the rainfall forecast using the WRF model.

Compared with Modes 6, 7 and 8, Modes 9, 10 and 11 also assimilated the GTS data in Domain 2 at the same time. The difference between the forecasted rainfall totals for Modes 6 and 9 was not significant, although Mode 9 performed worse than Mode 6. However, the relative error for Mode 10 was -58.74%, which was much higher than of Mode 7. This finding indicates that assimilating the GTS data over a small area (Domain 2) may have increased the forecast error, whereas the forecasted rainfall may not have been greatly influenced when the radar reflectivity was assimilated in Domain 2 at the same time. For Mode 11, the relative error (-3.77%) was the lowest among the 11 modes, which means that the improvement in the rainfall forecast was large and much closer to the rain gauge observations. This result indicates that assimilating the three types of observations (i.e., GTS data, radar reflectivity and radar velocity) at the same time is the best choice for rainfall forecast improvement. However more similar researches should be carried out to support the conclusion.

4.3 Influence of the number of assimilated observations

To further explore the assimilation techniques and the causes of the assimilation effects, the number of assimilated observations for each of the 11 modes is shown in Table 3.

[Table 3]

Mode 3 can be regarded as a combination of Modes 1 and 2. The number of assimilated observations in Mode 3 was less than the sum of the number of assimilated observations in Modes 1 and 2 at each time. Therefore, there was a conflict between the radar reflectivity and radial velocity, and some of the radar data were not assimilated in the WRF model when the two types of radar data were assimilated in the same domain at the same time. However, Mode 3 performed worse than Mode 1, which indicates that assimilating the radial velocity data in Domain 2 had a negative effect on the forecasted rainfall. For Modes 1, 2 and 4, the ranking of the number of assimilated observations was Mode 2 > Mode 1 > Mode 4, whereas the ranking of the performance from best to worst was Mode 4 > Mode 1 > Mode 2. This result indicates that the GTS data were more effective in data assimilation for the rainfall forecasts.

Through a comparative analysis of Modes 1 and 6, Modes 2 and 7, and Modes 3 and 8, Modes 6, 7 and 8 assimilated fewer observations than Modes 1, 2 and 3, although the assimilation effects were improved. This finding indicates that the data assimilation approach in Modes 6, 7 and 8 was more rational. The assimilation of the GTS data in Domain 1 helped eliminate the unreasonable radar data assimilated in Modes 1, 2 and 3 and improved the radar data assimilation results.

The comparisons were also made between Modes 6 and 9, Modes 7 and 10, and Modes 8 and 11. For Modes 9, 10 and 11, the number of assimilated observations in Domain 2 was more than for Modes 6, 7 and 8, which means that the GTS data were assimilated by the WRF model in Domain 2. However, the assimilation results indicate that more assimilated data did not mean better assimilation effects. Due to the assimilation of the GTS data in Domain 2, the rainfall forecasts of Modes 9 and 10 were worse than for Modes 6 and 7, respectively, whereas Mode 11, which had the lowest relative error, provided the best forecast among the 11 modes.

5 Discussion

Among the 11 data assimilation modes, assimilating radar velocity always led to poorer results than the original rainfall forecasts. The assimilation of radar velocity cannot directly influence the physical process of rainfall, although it can affect the water vapor transport via the atmospheric motions. However, if the assimilated radar velocity cannot improve the atmospheric circulation predictions, the water vapor field may not be improved, and thus the rainfall forecasts may also be found unimproved (Pan et al, 2012; Dong and Xue, 2013). In reality, the accuracy of the radial velocity data depends on the atmospheric refractive index, which is affected by the air density and the water vapor content (Montmerle and Faccani, 2010; Maiello et al, 2014). Unfortunately, both the air density and the water vapor content are quite variably, especially on rainy days (Abdalla and Cavaleri, 2002). Therefore, the spatial observation errors in the radial velocity retrievals are unavoidable and might be the main factor that leads to poorer performance of the NWP model than that achieved without data assimilation (Abhilash et al, 2012). Due to the frequent adjustment of the atmospheric motions, decreasing the assimilation time interval may reduce the risk of over correction (Xiao et al, 2005). However, the added information may involve more observation errors that will increase the nonlinearity of the atmosphere and make the model convergence more difficult. The radar used in this study had a temporal resolution of 0.1 h, whereas the assimilation time interval was 6 h; therefore, there is still room to increase the data assimilation frequency, although there is a trade-off between model performance and the operating efficiency.

Radar reflectivity data contain information related to the precipitation hydrometeors, and the assimilation of radar reflectivity data can directly influence the physical process of rainfall. In this study, assimilating radar reflectivity always had a positive effect on the forecasted rainfall, and the performance was relatively stable. In this study the data assimilation modes which involved the radar reflectivity always performed better than the others. It can also be found that the assimilation of the GTS data played a subsidiary role to the radar reflectivity in improving the rainfall forecasts. Although the GTS data itself cannot produce more prominent results than the radar reflectivity, a combination of the radar reflectivity together with the GTS data

always resulted in better results that assimilating the radar data alone. The involvement of the GTS data in the outer domain might be able to help improve the atmospheric state at a relatively large scale, which induces a positive effect on the rainfall forecasts in the inner domain.

In order to further verify the findings of the assimilation results, another two storm events with relatively moderate rainfall intensity (around 50mm for 24hr accumulation) were selected from an analogue catchment to be forecasted with four simplified assimilation modes (Mode 1, 3, 4, 6). The analogue catchment locates in the southern reach of the Daqing river basin with a drainage area of 2210 km^2. Table 4 shows the details of the storm events and the rainfall forecasting results from different data assimilation modes. The cumulative curves of the forecasted areal rainfall are illustrated in Figure 6. Results were found to in accordance with the conclusions from the extreme event in Zijingguan catchment. Assimilating radar reflectivity together with radial velocity (Mode 3) cannot guarantee improved results than only assimilating radar reflectivity (Mode 1). The GTS data alone can also generate as good results (Mode 4) as the radar reflectivity. When the radar reflectivity is assimilated in the inner domain, the involvement of the GTS data in the outer domain (Mode 6) further helped produce better results.

[Figure 6 and Table 4]

6 Conclusion

This study explored the effects of data assimilation using WRF-3DVar for the improvement of rainfall forecasting in the Beijing-Tianjin-Hebei region of Northern China. Two nested domains were employed, and the GFS data were used to drive the WRF model. A storm event that occurred over the Beijing-Tianjin-Hebei region on 21 July 2012 was selected, considering the widespread attention it received in China due to the high intensity, wide coverage of the rainfall process and the significant losses caused by the following flood. The rainfall accumulation during the storm in a mountainous catchment named Zijingguan with a drainage area of 1760 km^2 was set as the forecasting target. Three types of observations, i.e., GTS data, radar reflectivity and radial velocity, were used to investigate the potential improvements on WRF rainfall forecasts through data assimilation. Eleven data assimilation modes were designed based on different combinations of the three types of observations in the two nested domains.

Contrastive analyses of the rainfall forecasts from the 11 data assimilation modes were carried out from three aspects: the rainfall evolution process, the accumulated amount and the number of the observations assimilated. Four main conclusions can be drawn: 1) when the radar data was assimilated alone, the assimilation of radar reflectivity performed better than radial velocity in improving the rainfall forecasts, and the assimilation of both two types of the radar data generated poorer results than only assimilating the radar reflectivity; 2) the assimilation of the GTS data can also improve the rainfall forecasts, and its assimilation efficiency was the highest among the three types of observations, indicating that relatively accurate rainfall forecasts can be achieved by assimilating only a small amount of data; 3) the combination of GTS and radar data resulted in

the best improvements of the rainfall forecasts, and, in particular, the involvement of the GTS data in the outer domain when radar data are assimilated in the inner domain resulted in better forecasts than only assimilating the radar data; 4) assimilating more observations does not guarantee further improvement, on the other hand, the effective information contained in the assimilated data is of more importance than the data quantity. In this study, the involvement of the GTS data when both the radar reflectivity and radial velocity were assimilated in the innermost domain provided the most obvious improvements. Considering the poor performance of radial velocity in other assimilation modes and the reasons explained in the discussion, the radial velocity data should be carefully used with a very strict quality control process. Further research considering various geographical and meteorological case studies should be carried out to further verify the conclusions of this study.

Author Contributions

All the authors contributed to conception and development of this manuscript under the supervision of Denghua Yan and Fuliang Yu, specifically Jia Liu and Jiyang Tian carried out the calculations and analysis of the results. Chuanzhe Li,and Feifei Shen designed the framework and checked the English writing.

Acknowledgements

This study was supported by the National Key Research and Development Program (Grant No. 2016YFA0601503), the Major Science and Technology Program for Water Pollution Control and Treatment (Grant No. 2018ZX07110001), the National Natural Science Foundation of China (Grant No. 51409270), the Hebei Province Water Scientific Research Project (Grant No. 2015-16), and the IWHR Research & Development Support Program (Grant No. WR0145B732017).

Competing interests: The authors declare that they have no conflict of interest.

References

Abdalla, S., and Cavaleri, L.: Effect of wind variability and variable air density on wave modelling, J. Geophys. Res., 107, 17-1-17-17., doi: 10.1029/2000JC000639, 2002.

Abhilash, S., Sahai, A. K., Mohankumar, K., George, J. P., and Das, S.: Assimilation of doppler weather radar radial velocity and reflectivity observations in WRF-3DVAR system for short-range forecasting of convective storms, Pure Appl. Geophys., 169, 2047-2070, doi: 10.1007/s00024-012-0462-z, 2012.

Barker, D. M., Huang, W., Guo, Y. R., Bourgeois, A., and Xiao, Q. N.: A three-dimensional variational data assimilation systemfor MM5: implementation and initial results, Mon. Weather Rev., 132, 897–914, doi: 10.1175/1520-0493(2004)132<0897:ATVDAS>2.0.CO;2, 2004.

Bauer, H. S., Schwitalla, T., Wulfmeyer, V., Bakhshall, A., Ehret, U., Neuper, M., and Caumont, O.: Quantitative precipitation estimation based on high-resolution numerical weather prediction and data assimilation with WRF-a performance test, Tellus A., 67, doi: 10.3402/tellusa.v67.25047, 2015.

Berenguer, M., Surcel, M., Zawadzki, I., Xue, M., and Kong, F.: The diurnal cycle of precipitation from continental radar mosaics and numerical weather prediction models. Part II: Intercomparison among numerical models and with nowcasting, Mon. Weather Rev., 140, 2689-2705, doi: 10.1175/MWR-D-11-00181.1, 2012.

Boussetta, S., Balsamo, G., Beljaars, A., and Kral, T.: Impact of a satellite-derived Leaf Area Index monthly climatology in a global Numerical Weather Prediction model, Int. J. Remote Sens., 34, 3520-3542, doi: 10.1080/01431161.2012.716543, 2013.

Chambon, P., Zhang, S. Q., Hou, A. Y., Zupanski, M., and Cheung, S.: Assessing the impact of pre-GPM microwave precipitation observations in the Goddard WRF ensemble data assimilation system, Q. J. Roy. Meteor Soc., 140, 1219–1235. doi: 10.1002/qj.2215, 2014.

Di, Z., Duan, Q., Gong, W., Wang, C., Gan, Y., Quan, J., Li, J., Miao, C., Ye, A., and Charles, T.: Assessing WRF model parameter sensitivity: A case study with 5 day summer precipitation forecasting in the Greater Beijing Area, Geophys. Res. Lett., 42, 579-587, doi: 10.1002/2014GL061623, 2015.

Dong, J., and Xue, M.: Assimilation of radial velocity and reflectivity data from coastal WSR-88D radars using an ensemble Kalman filter for the analysis and forecast of landfalling hurricane Ike (2008), Q. J. Roy. Meteor. Soc., 139, 467-487, doi: 10.1002/qj.1970, 2013.

Efstathiou, G. A., Zoumakis, N. M., Melas, D., Lolis, C. J., and Kassomenos, P.: Sensitivity of WRF to boundary layer parameterizations in simulating a heavy rainfall event using different microphysical schemes, Effect on large-scale processes, Atmos. Res., 132, 125-143, doi: 10.1016/j.atmosres.2013.05.004, 2013.

Fernández-González, S., Valero, F., Sánchez, J. L., Gascón, E., López, L., García-Ortega, E., and Merino, A.: Numerical simulations of snowfall events: Sensitivity analysis of physical parameterizations, J. Geophys. Res. Atmos., 120, 10130-10148, doi: 10.1002/2015JD023793, 2015.

Gao, J. D., Xue, M., Brewster, K. A., and Droegemeier, K.: A three-dimensional variational data analysis method with recursive filter for Doppler radars, J. Atmos. Oceanic Technol., 21, 457-469, doi: 10.1175/1520-0426(2004)021<0457:ATVDAM>2.0.CO;2, 2004.

Gascón, E., Laviola, S., Merino, A., and Miglietta, M. M.: Analysis of a localized flash-flood event over the central Mediterranean, Atmos. Res., 182, 256-268, doi: 10.1016/j.atmosres.2016.08.007, 2016.

Giorgi, M. G. D., Ficarella, A., and Tarantino, M.: Assessment of the benefits of numerical weather predictions in wind power forecasting based on statistical methods, Energy, 36, 3968-3978, doi: 10.1016/j.energy.2011.05.006, 2011.

Guo, X., Fu, D., Guo, X., and Zhang, C.: A case study of aerosol impacts on summer convective clouds and precipitation over northern China, Atmos. Res., 142, 142-157, doi: 10.1016/j.atmosres.2013.10.006, 2014.

Ha, J. H., and Lee, D. K.: Effect of length scale tuning of bachground error in WRF-3DVar system on assimilation of high-resolution surface data for heavy rainfall simulation, Adv. Atmos. Sci., 29, 1142-1158, doi: 10.1007/s00376-012-1183-z, 2012.

Ha, J. H., Lim, G. H., Choi, S. J.: Assimilation of GPS radio occultation refractivity data with WRF 3DVAR and its impact on the prediction of a heavy rainfall event, J. Appl. Meteorol. Clim., 53, 1381-1398, doi: 10.1175/JAMC-D-13-0224.1, 2014.

Hamill, T. M.: Performance of Operational model precipitation forecast guidance during the 2013 Colorado front-range floods, Mon. Weather Rev., 142, 2609-2618, doi: 10.1175/MWR-D-14-00007.1, 2014.

Hunter, S. M.: WSR-88D radar rainfall estimation: Capabilities, limitations and potential improvements, Natl. Wea. Dig., 20, 26-38, 1996.

Ide, K., Courtier, P., Ghil, M., Lorenc, A. C.: Unified Notation for data assimilation: Operational, sequential and variational, J. Meteorol. Soc. Jpn., 75, 181-189, 1997.

Kryza, M., Werner, M., Wałszek, K., and Dore, A. J.: Application and evaluation of the WRF model for high-resolution forecasting of rainfall–a case study of SW Poland, Meteorol. Z., 22, 595-601, doi: 10.1127/0941-2948/2013/0444, 2013.

Li, D., Bouzeid, E., Baeck, M. L., Jessup, S., and Smith, J. A.: Modeling land surface processes and heavy rainfall in urban environments: Sensitivity to urban surface representations, J. Hydrometeorol., 14, 1098-1118, doi: 10.1175/JHM-D-12-0154.1, 2013.

Li, Y., Wang, X., and Xue, M.: Assimilation of radar radial velocity data with the WRF hybrid ensemble–3DVAR system for the prediction of Hurricane Ike (2008), Mon. Weather Rev., 140, 3507-3524, doi: 10.1175/MWR-D-12-00043.1, 2012.

Lin, H. H., Lin, P. L., Xiao, Q., and Kuo, Y. H.: Effect of Doppler radial velocity data assimilation on the simulation of a typhoon approaching Taiwan: A case study of Typhoon Aere (2004), Terr. Atmos. Ocean. Sci., 22, 325-345, doi: 10.3319/TAO.2010.10.08.01(A), 2011.

Liu, J., Bray, M., and Han, D.: Sensitivity of the Weather Research and Forecasting (WRF) model to downscaling ratios and storm types in rainfall simulation, Hydrol. Process., 26, 3012-3031, doi: 10.1002/hyp.8247, 2012.

Liu, J., Bray, M., and Han, D.: A study on WRF radar data assimilation for hydrological rainfall precipitation, Hydro. Earth Syst. Sci., 17, 3095-3110, doi: 10.5194/hess-17-3095-2013, 2013.

Liu, J., Bray, M., and Han, D.: Exploring the effect of data assimilation by WRF-3DVar for numerical rainfall prediction with different types of storm events, Hydrol. Process., 27, 3627-3640, doi: 10.1002/hyp.9488, 2013.

Liu, J., and Han, D.: On selection of the optimal data time interval for real-time hydrological forecasting, Hydro. Earth Syst. Sci., 17, 3639-3659, doi: 10.5194/hess-17-3639-2013, 2013.

Liu, J., Wang, J., Pan, S., Tang, K., Li, C., and Han, D.: A real-time flood forecasting system with dual updating of the NWP rainfall and the river flow, Nat. Hazards., 77, 1161-1182, doi: 10.1007/s11069-015-1643-8, 2015.

Maiello, I., Ferretti, R., Gentile, S., Montopoli, M., Picciotti, E., Marzano, F. S., and Faccani, C.: Impact of radar data assimilation for the simulation of a heavy rainfall case in central Italy using WRF–3DVAR, Atmos. Meas. Tech., 7, 2919-2935, doi: 10.5194/amt-7-2919-2014, 2014.

Meng, Z., and Zhang, F.: Tests of an ensemble Kalman filter for mesoscale and regional-scale data assimilation, Part IV: Comparison with 3DVAR in a month-long experiment, Mon. Weather Rev., 136, 3671-3682, doi: 10.1175/2007MWR2106.1, 2008.

Miao, S., Chen, F., and Li, Q.: Impacts of urban processes and urbanization on summer precipitation: A case study of heavy rainfall in Beijing on 1 August 2006, J. Appl. Meteorol. Clim., 50, 806-825, doi: 10.1175/2007MWR2106.1, 2011.

Mohanty, U. C., Routray, A., Osuri, K. K., and Prasad, S. K.: A study on simulation of heavy rainfall events over Indian region with ARW-3DVAR modeling system, Pure. Appl. Geophys., 169, 381-399, doi: 10.1007/s00024-011-0376-1, 2012.

Montmerle, T., and Faccani, C.: Mesoscale assimilation of radial velocities from Doppler radars in a preoperational framework, Mon. Weather Rev., 137, 1939-1953, doi: 10.1175/2008MWR2725.1, 2010.

Pan, X., Tian, X., Li, X., Xie, Z., Shao, A., and Lu, C.: Assimilating Doppler radar radial velocity and reflectivity observations in the weather research and forecasting model by a proper orthogonal-decomposition-based ensemble, three-dimensional variational assimilation method, J. Geophys. Res. Atmos., 117, D17113, doi: 10.1029/2012JD017684, 2012.

Pu, Z., Li, X., and Sun, J.: Impact of airborne Doppler radar data assimilation on the numerical simulation of intensity changes of Hurricane Dennis near a landfall, J. Atmos. Sci., 66, 3351-3365, doi: 10.1175/2009JAS3121.1, 2009.

Qie, X., Zhu, R., Yuan, T., Wu, X., Li, W., and Liu, D.: Application of total-lightning data assimilation in a mesoscale convective system based on the WRF model, Atmos. Res., 145–146, 255-266, doi: 10.1016/j.atmosres.2014.04.012, 2014.

Rodwell, M. J., Richardson, D. S., Hewson, T. D., and Haiden, T.: A new equitable score suitable for verifying precipitation in numerical weather prediction, Q. J. Roy. Meteor. Soc., 136, 1344-1363, doi: 10.1002/qj.65, 2010.

Routray, A., Mohanty, U. C., Niyogi, D., Rizvi, S. R. H., and Osuri, K. K.: Simulation of heavy rainfall events over Indian monsoon region using WRF-3DVAR data assimilation system, Meteorol. Atmos. Phys., 106, 107-125, doi: 10.1007/s00703-009-0054-3, 2010.

Routray, A., Osuri, K. K., and Kulkarni, M. A.: A comparative study on performance of analysis nudging and 3DVAR in simulation of a heavy rainfall event using WRF modeling system, Isrn. Meteorology., 2012, 1191-1213, doi: 10.5402/2012/523942, 2012.

Shrestha, D. L., Robertson, D. E., Wang, Q. J., Pagano, T. C., and Hapuarachchi, H. A. P.: Evaluation of numerical weather prediction model precipitation forecasts for short-term streamflow forecasting purpose, Hydrol. Earth. Syst. Sc., 17, 1913-1931, doi: 10.5194/hess-17-1913-2013, 2013.

Skamaraock, W. C., Klemp, J. B., Dudhia, J., Gill, D. O., Barker, D. M., Duda, M. G., Huang, X. Y., Wang, W., and Powers, J. G.: A description of the advanced research WRF Version 3, NCAR technical note, Available from http://www.ncar.ucar.edu, 2008.

Sugimoto, S., Crook, N. A., Sun, J., Xiao, Q., and Barker, D. M.: An examination of WRF 3DVAR radar data assimilation on its capability in retrieving unobserved variables and forecasting precipitation through observing system simulation experiments, Mon. Weather Rev., 137, 4011-4029, doi: 10.1175/2009MWR2839.1, 2009.

Sun, J., Trier, S. B., Xiao, Q., Weisman, M. L., Wang, H., Ying, Z., Xu, M., and Zhang, Y.: Sensitivity of 0-12-h warm-season precipitation forecasts over the central United States to model initialization, Weather Forecast., 27, 832-855, doi: 10.1175/WAF-D-11-00075.1, 2012.

Tong, M., and Xue, M.: Ensemble Kalman filter assimilation of Doppler radar data with a compressible nonhydrostatic model: OSS Experiments, Mon. Weather Rev., 133, 1789–1807, doi: 10.1175/MWR2898.1, 2005.

Xiao, Q., Kuo, Y. H., Sun, J., Lee, W. C., Lim, E., Guo, Y. R., and Barker, D. M.: Assimilation of Doppler radar observations with a regional 3DVAR System: Impact of Doppler velocities on forecasts of a heavy rainfall case, J. Appl. Meteorol., 44, 768-788, doi: 10.1175/JAM2248.1, 2005.

Xiao, Q., and Sun, J.: Multiple-radar data assimilation and short-range quantitative precipitation forecasting of a squall line observed during, IHOP_2002, Mon. Weather Rev., 135, 3381-3404, doi: 10.1175/MWR3471.1, 2007.

Yang, B., Zhang, Y., and Qian, Y.: Simulation of urban climate with high-resolution WRF model: A case study in Nanjing, China, ASIA-PAC. J. Atmos. Sci., 48, 227-241, doi: 10.1007/s13143-012-0023-5, 2012.

Yang, B., Zhang, Y., Qian, Y., Huang, A., and Yan, H.: Calibration of a convective parameterization scheme in the WRF model and its impact on the simulation of East Asian summer monsoon precipitation, Clim. Dynam., 44, 1661-1684, doi: 10.1007/s00382-014-2118-4, 2015.

Zhang, L., Pu, Z., Lee, W. C., and Zhao, Q.: The influence of airborne Doppler radar data quality on numerical simulations of a tropical cyclone, Weather Forecast., 27, 231-239, doi: 10.1175/WAF-D-11-00028.1, 2012.

Table captions

Table 1: Assimilation modes of different data combinations.

Table 2: 24 h accumulated areal rainfall observations and forecasts.

Table 3: Total number of assimilated observations in the two nested domains.

Table 4: The two storm events of the analogue catchment and the relative errors of the rainfall forecasts with/without data assimilation.

Figure captions

Figure 1: The location of the Zijingguan catchment with the 11 rain gauges (a) and 3×3 km grid cells (b).

Figure 2: Relative positions of the radar scan area and the nested domains.

Figure 3: Comparison of the rainfalls from the rain gauges and radar: (a) time series bars of the hourly catchment areal rainfall; (b) 24 h rainfall accumulation from the rain gauges; (c) 24 h rainfall accumulation from the radar.

Figure 4: The time bars of the cycling WRF-3DVar runs.

Figure 5: Cumulative curves of rainfall for the eleven data assimilation modes.

Figure 6: Rainfall cumulative curves of the two storm events in the analogue catchments with different data assimilation modes.

Hydrol. Earth Syst. Sci. Discuss., https://doi.org/10.5194/hess-2017-689
Manuscript under review for journal Hydrol. Earth Syst. Sci.
Discussion started: 2 January 2018

Hydrology and Earth System Sciences
Discussions

Table 1. Assimilation modes of different data combinations

Modes	Assimilated data	
	Domain 1	Domain 2
1	/	radar reflectivity
2	/	radial velocity
3	/	radar reflectivity and radial velocity
4	GTS data	/
5	GTS data	GTS data
6	GTS data	radar reflectivity
7	GTS data	radial velocity
8	GTS data	radar reflectivity and radial velocity
9	GTS data	GTS data and radar reflectivity
10	GTS data	GTS data and radial velocity
11	GTS data	GTS data, radar reflectivity, and radial velocity

Hydrol. Earth Syst. Sci. Discuss., https://doi.org/10.5194/hess-2017-689
Manuscript under review for journal Hydrol. Earth Syst. Sci.
Discussion started: 2 January 2018

Hydrology and Earth System Sciences
Open Access
EGU
Discussions

Table 2. 24 h accumulated areal rainfall observations and forecasts

Modes	Rain gauge (mm)	WRF model (mm)	Relative error (%)
No data assimilation	172.17	95.54	-44.51
1	172.17	118.92	-30.93
2	172.17	77.65	-54.90
3	172.17	79.76	-53.67
4	172.17	129.02	-25.06
5	172.17	111.71	-35.11
6	172.17	136.37	-20.79
7	172.17	132.89	-22.82
8	172.17	132.89	-22.81
9	172.17	124.74	-27.55
10	172.17	71.04	-58.74
11	172.17	165.68	-3.77

Hydrol. Earth Syst. Sci. Discuss., https://doi.org/10.5194/hess-2017-689
Manuscript under review for journal Hydrol. Earth Syst. Sci.
Discussion started: 2 January 2018

Hydrology and Earth System Sciences
Discussions

Table 3. Total number of assimilated observations in the two nested domains

Modes	Domain	Number of assimilated observations				
		Time 1	Time 2	Time 3	Time 4	Time 5
		21/07 00:00	21/07 06:00	21/07 12:00	21/07 18:00	22/07 00:00
1	1	/	/	/	/	/
	2	16158	19233	26032	11821	6239
2	1	/	/	/	/	/
	2	75014	107901	57095	60993	23508
3	1	/	/	/	/	/
	2	60550	84573	71148	45896	24924
4	1	2625	1758	2445	930	723
	2	/	/	/	/	/
5	1	2625	1758	2445	930	723
	2	596	170	304	145	106
6	1	2625	1758	2447	931	720
	2	6156	2905	14795	3795	4232
7	1	2625	1760	2450	934	721
	2	54394	14954	40227	52914	20984
8	1	2625	1760	2450	931	724
	2	60550	17806	72966	39142	23912
9	1	2625	1759	2444	937	723
	2	6752	3095	31711	42108	20194
10	1	2625	1758	2446	935	719
	2	54990	64247	78253	53209	24628
11	1	2625	1760	2449	941	725
	2	61146	17823	74014	41592	24293

Hydrol. Earth Syst. Sci. Discuss., https://doi.org/10.5194/hess-2017-689
Manuscript under review for journal Hydrol. Earth Syst. Sci.
Discussion started: 2 January 2018

Table 4. The two storm events of the analogue catchment and the relative errors of the rainfall forecasts with/without data assimilation

Event	Duration	Rain gauge observation (mm)	WRF original run (%)	Assimilation results (%)			
				Mode 1	Mode 3	Mode 4	Mode 6
a	29/07/2007 20:00-30/07/2007 20:00	63.38	-15.94	-11.45	-14.66	-9.35	-2.78
b	30/07/2012 10:00-31/07/2012 10:00	50.48	-26.26	-9.69	-17.16	-6.01	-2.10

Hydrol. Earth Syst. Sci. Discuss., https://doi.org/10.5194/hess-2017-689
Manuscript under review for journal Hydrol. Earth Syst. Sci.
Discussion started: 2 January 2018

Hydrology and Earth System Sciences
Discussions
Open Access
EGU

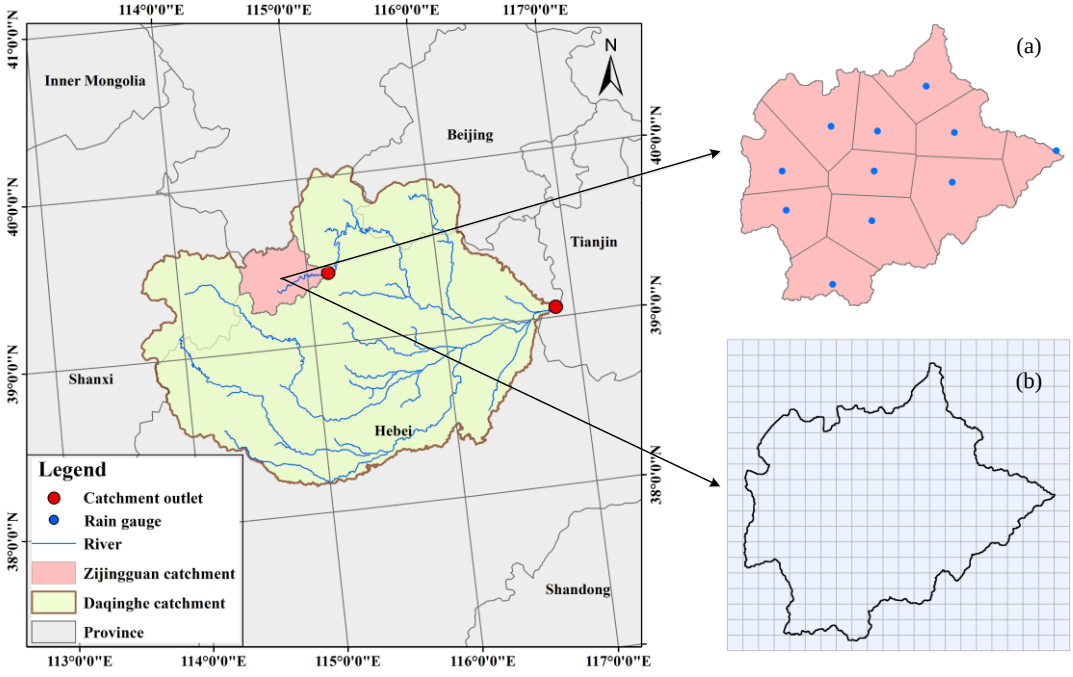

Figure 1. The location of the Zijingguan catchment with the 11 rain gauges (a) and 3×3 km grid cells (b).

Hydrol. Earth Syst. Sci. Discuss., https://doi.org/10.5194/hess-2017-689
Manuscript under review for journal Hydrol. Earth Syst. Sci.
Discussion started: 2 January 2018

Hydrology and Earth System Sciences
Discussions

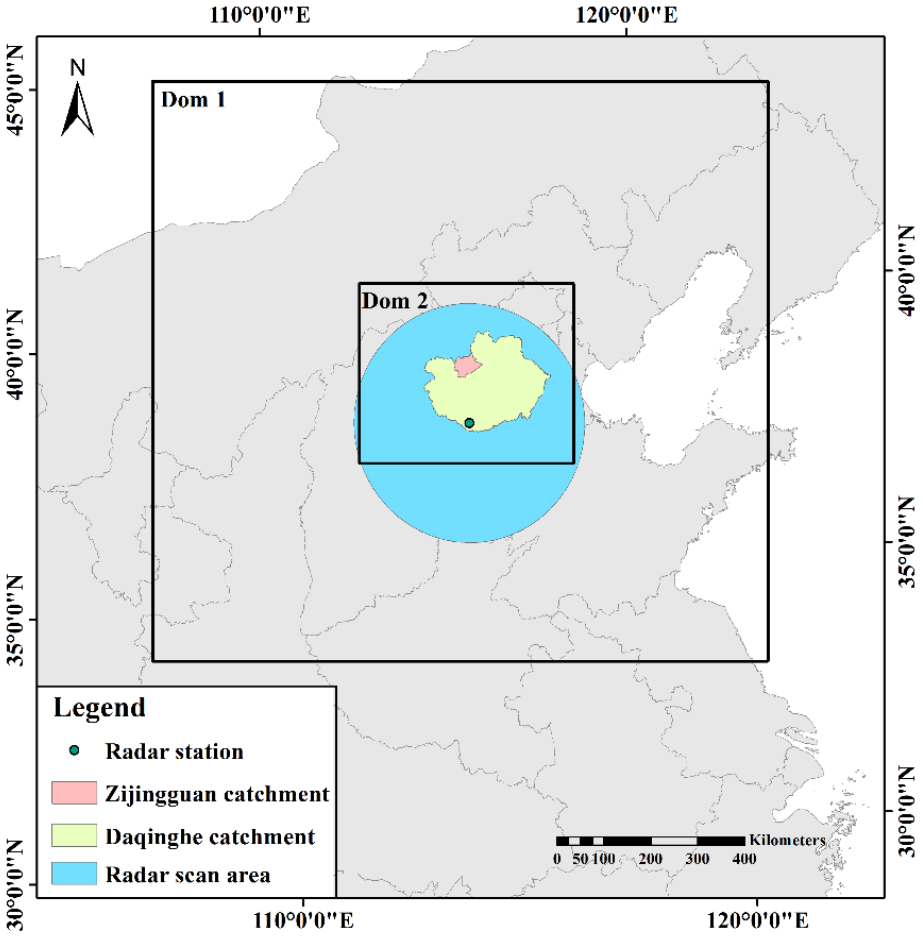

Figure 2. Relative positions of the radar scan area and the nested domains.

Hydrol. Earth Syst. Sci. Discuss., https://doi.org/10.5194/hess-2017-689
Manuscript under review for journal Hydrol. Earth Syst. Sci.
Discussion started: 2 January 2018

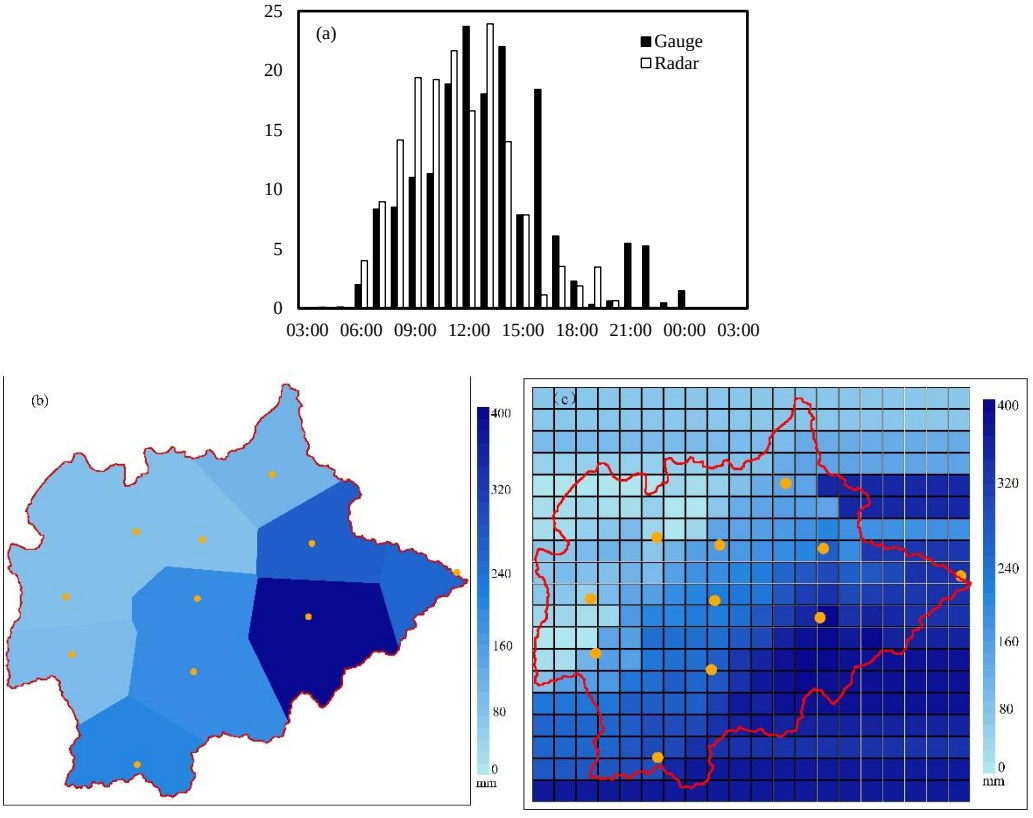

Figure 3. Comparison of the rainfalls from the rain gauges and radar: (a) time series bars of the hourly catchment areal rainfall; (b) 24 h rainfall accumulation from the rain gauges; (c) 24 h rainfall accumulation from the radar.

Hydrol. Earth Syst. Sci. Discuss., https://doi.org/10.5194/hess-2017-689
Manuscript under review for journal Hydrol. Earth Syst. Sci.
Discussion started: 2 January 2018

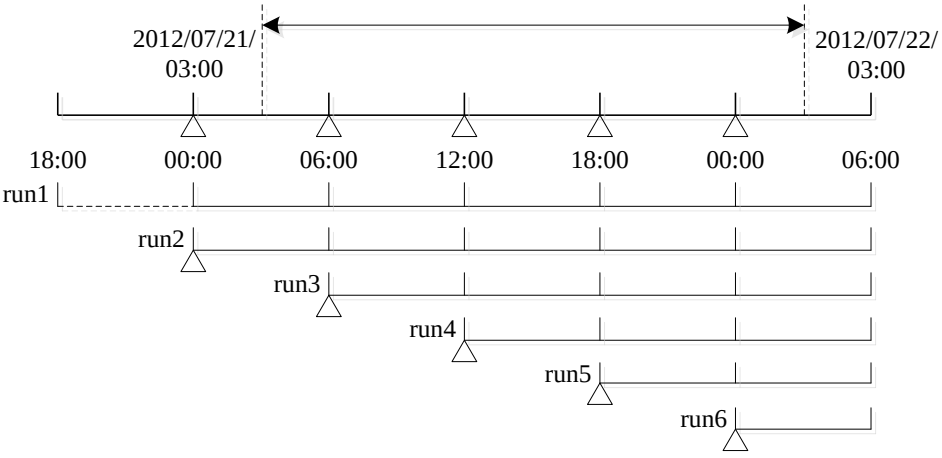

Figure 4. The time bars of the cycling WRF-3DVar runs.

Hydrol. Earth Syst. Sci. Discuss., https://doi.org/10.5194/hess-2017-689
Manuscript under review for journal Hydrol. Earth Syst. Sci.
Discussion started: 2 January 2018

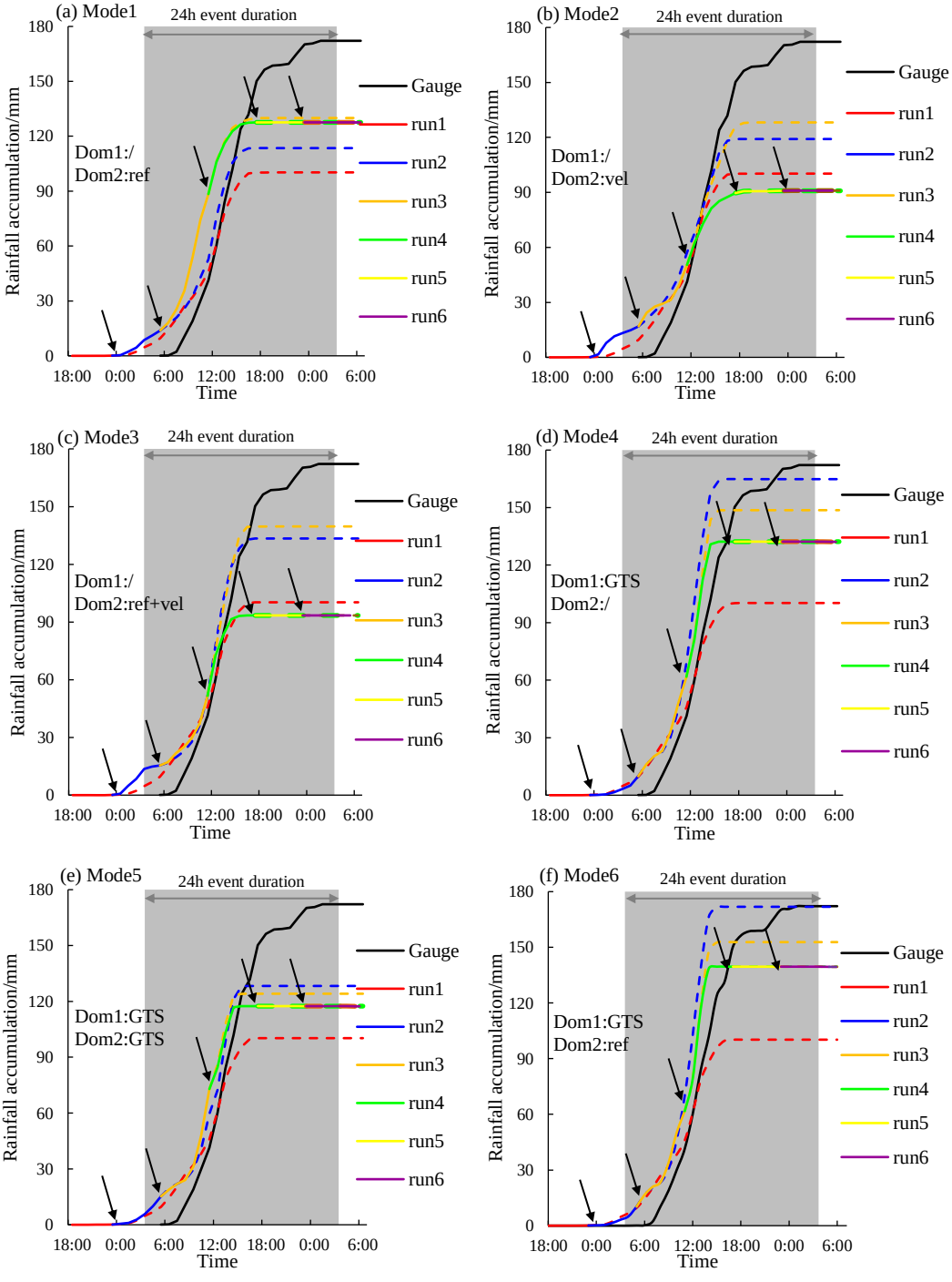

Hydrol. Earth Syst. Sci. Discuss., https://doi.org/10.5194/hess-2017-689
Manuscript under review for journal Hydrol. Earth Syst. Sci.
Discussion started: 2 January 2018

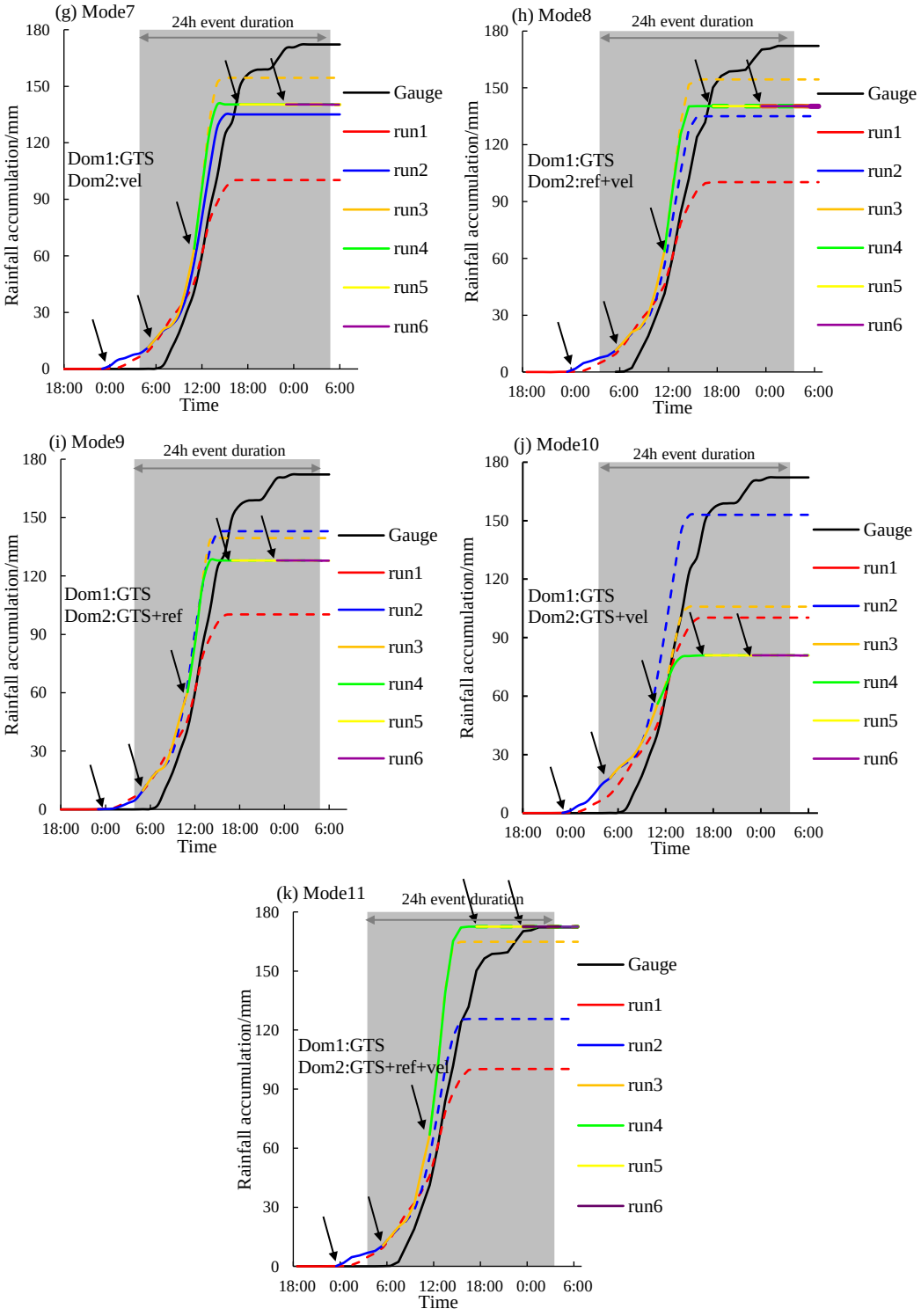

Figure 5. Cumulative curves of rainfall for the eleven data assimilation modes.

Hydrol. Earth Syst. Sci. Discuss., https://doi.org/10.5194/hess-2017-689
Manuscript under review for journal Hydrol. Earth Syst. Sci.
Discussion started: 2 January 2018

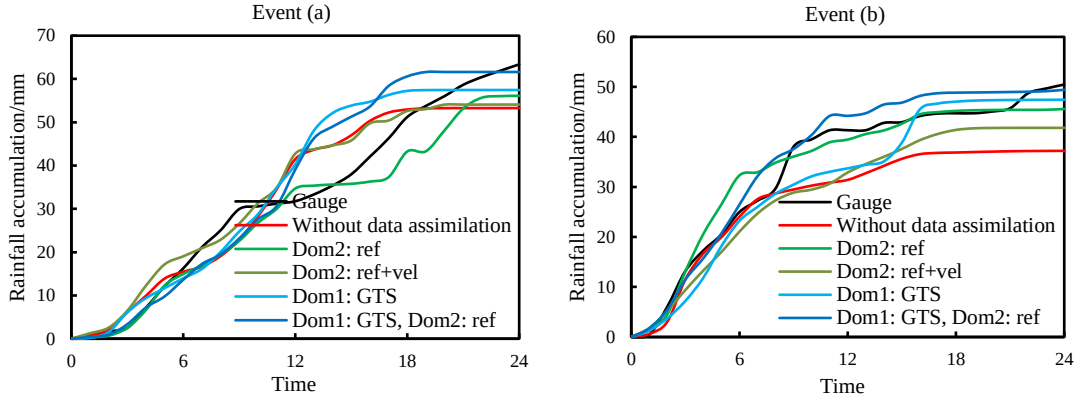

Figure 6. Rainfall cumulative curves of the two storm events in the analogue catchments with different data assimilation modes.